Effect of Halogen in High-Density Oxygen Plasmas on Photoresist Trimming

Chian-Yuh Sin
Dept. of Chemical and Biomolecular Engineering, National University of Singapore, Singapore 119260

and

Chartered Semiconductor Manufacturing Ltd., Singapore 738406

Bing-Hung Chen
Dept. of Chemical and Biomolecular Engineering, National University of Singapore, Singapore 119260

and

Dept. of Chemical Engineering, National Cheng Kung University, 1 University Road, Taiwan 70101, Taiwan

W. L. Loh, J. Yu, P. Yelehanka, A. See, and L. Chan
Chartered Semiconductor Manufacturing Ltd., Singapore 738406

DOI 10.1002/aic.10145
Published online in Wiley InterScience (www.interscience.wiley.com).

Effects of halogens, CF_4, Cl_2, or HBr, on the photoresist trimming in high-density oxygen plasmas for sub-0.1-μm device fabrication were studied in an inductively coupled plasma (ICP) etcher. The trim rates were measured as a function of halogen gas percentages. The activation energy and the resulting resist profiles were investigated as well, showing that the CF_4/O_2 gives the highest trim rate, followed by HBr/O_2 and then Cl_2/O_2 at the same amount of additive gas in the mixture. Effects of different plasma chemistry on the chemical constituents of the resist sidewall films were also examined with the angle-resolved X-ray photoelectron spectroscopy (XPS). XPS analysis reveals that all halogen gases are useful for resist sidewall protection because of the passivation by the halogen-containing polymer. The effects of halogen addition include the reaction enhancement, reaction-site competition between oxygen and halogen, changes in the plasma gas chemistry, and the resist passivation. © 2004 American Institute of Chemical Engineers *AIChE J,* 50: 1578–1588, 2004
Keywords: photoresist trimming, oxygen plasma, halogen, ICP etcher, activation energy, trim rate, resist profiles

Introduction

The relentless drive in the integrated circuit industry toward greater packing density and higher speeds has served as the momentum to reduce the device dimensions. The fabrication of ever-smaller integrated circuit devices is closely related to developments in patterning technologies (that is, lithography and etching). The corresponding reduction in feature size is usually accompanied by the reduction in wavelength used in lithography as noted in the International Technology Roadmap for Semiconductors (ITRS). However, the much more aggressive requirements on the ultrasmall gate features necessitate

Correspondence concerning this article should be addressed to B.-H. Chen at bhchen@alumni.rice.edu.

much smaller resolution limit than could be reached by the current lithography tools available for manufacturing (Peters, 2003).

Although the lithography tools for ultrasmall gate printing are not yet available, one possible way to obtain such small devices is through modification in the dry etching scheme. The new strategy proposed to make gate transistors less than the resolution allowed is to reduce the critical dimension (CD) of the photoresist feature, to be used as the etch mask, before the subsequent procedures of the polysilicon gate etching. The final critical dimension of the polysilicon gate is thus determined by the trimmed amount of the photoresist (Sin et al., 2002).

Similar techniques to reduce the linewidth of the masking materials have also been described as "photoresist ashing" (Chung et al., 1988), "oxide lateral etching" (Burmester et al., 1991), or "resist thinning" (Lee et al., 1997; Nakao et al., 2000; Ono et al., 1995), and have been successfully used to fabricate n-type metal–oxide–semiconductor field effect transistors (MOSFETs) with effective channel length as small as 40 nm using deep ultraviolet (DUV) lithography (Ono et al., 1995). All these processes have the advantage of reducing the gate length without increasing the complexity of the lithography requirements. Studies have shown that resist trimming is both reproducible and uniform, and could be a viable technique for deep submicron device manufacturing (Baker et al., 2000; Burmester et al., 1991; Chung et al., 1988; Ono et al., 1995). It is worth noting that the etching is on the top-down direction of the feature, whereas the trimming is the etching on the lateral side of the device.

For a plausible application in the semiconductor industry, not only reasonable trim rate and high etch selectivity, but also good vertical profile of the feature, have to be achieved together during the resist trimming process. Vertical profile is especially important in controlling the critical dimension of the feature. It is known that the oxygen plasmas could provide good etch capability on the organic dielectric (Hsu et al., 2000), as well as very high removal rate of the organic resist and the high etching selectivity over the polysilicon and gate oxide. Furthermore, it has been reported that N_2, He, CHF_3 (Doemling, et al., 1998), Cl_2 (Kure et al., 1991; Sparks et al., 1992), HBr (Kure et al., 1991; Tokashiki et al., 1993), and SO_2 (Hutton et al., 1995; Pons et al., 1994) are also effective for dry development of resist.

In most cases, vertical profiles are obtained by adding a second constituent that is known for passivation formation, such as halogen-containing gas, to protect the sidewalls against further etching. Sometimes the second constituent is also added to the plasma to slow down the spontaneous reaction between the oxygen and the photoresist. Commonly, fluorocarbons are added to form passivation layers on the feature to maintain the vertical profiles (Doemling et al., 1998; Hsu et al., 2000; Li et al., 2002; Sin et al., 2002).

However, there is not much work that could be found in the literature on the mechanism and characteristics of the resist trimming process. Process optimization requires an understanding of the trimming mechanisms of the organic resist (Sin et al., 2002, 2003) as well as the effect of different chemistry on the trimming performance. Thus, the aim of this work is to investigate the effects of different gas chemistry in plasmas on the characteristic of the resist trimming.

In this project, the halogen-containing gas added to the oxygen plasmas is HBr, Cl_2, or CF_4. The resist trimming process is integrated with the etching and opening step of the organic bottom antireflective coating (BARC). Without breaking the vacuum in the same etcher, the subsequent etching process of the polysilicon gate electrode is then performed using the trimmed resist/BARC as an etch mask. Our previous study successfully illustrated the fabrication of the 80-nm gate length transistors using the 248-nm lithography (Sin et al., 2002, 2003)

In this study, the characteristics of resist trimming—the trim rate and the resist profile—are examined for the two-component halogen–O_2 mixtures (HBr/O_2, Cl_2/O_2, and CF_4/O_2). The activation energy of trimming in different gas chemistry is also determined. Angle-resolved X-ray photoelectron spectroscopy (XPS) is also used in an attempt to identify the correlations between the characteristics of the photoresist trimming processes and the chemical constituents of the sidewall passivation films of the photoresist formed in the HBr/O_2, Cl_2/O_2, and CF_4/O_2 plasmas. The results are compared and discussed to shed light on a better understanding of the photoresist trimming process mechanisms.

Experimental Methods

The high-density and low-pressure plasma used for resist trimming was generated by an inductively coupled plasma (ICP) source (TCP9400DFM, Lam Research), excited using a 13.56-MHz RF power supply. The wafer was biased with an additional 13.56 MHz RF power source. For an ICP system, plasma density and ion energy can be independently controlled by adjusting the RF source power as well as the RF bias voltage. The theory and characteristics of ICP plasma source were previously described by Keller et al. (1996). To provide good thermal conductance between the wafer and the susceptor, wafer clamping and helium backside cooling were used. In this study, all the trimming and etching were carried out at 70°C. Reactant gases were introduced into the etcher from the center of the chamber. Gas flow rate and chamber pressure can be controlled independently by adjusting the mass flow rate controller and throttle valve.

In this study, patterned 200-mm wafers masked with chemically amplified photoresist (CAR) were used. The gate stack consisted of a very thin gate oxide and doped polysilicon of 200 nm. Bottom antireflective coating (BARC) of 60 nm and chemically amplified resist film of 425 nm were subsequently spin-coated onto the polysilicon film. Conventional 248-nm lithography (KrF laser) was used to pattern the resist lines down to 0.12 μm. Resist trimming was then performed using the oxygen–halogen plasmas in the aforementioned ICP etcher. With the trimmed resist as an etch mask, etching of the polysilicon was processed in the same ICP etcher using HBr/Cl_2 plasma. That is, the BARC opening is performed simultaneously with the photoresist trimming process. Our previous study on the photoresist trimming technique, using CF_4/O_2 plasmas, indicates the optimal operation conditions for such a process could be preferably set as (1) 100 sccm (standard cm^3/min) CF_4 and 30 sccm O_2 (that is, 77% of halogen in the mixture); and (2) 70% overetch (Sin et al., 2003). Therefore, the operating conditions in this study include a 250-W source

power, −50-V bias voltage, 10 mTorr pressure, and 130 sccm for the total gas flow rate.

The test structures used for the study of trimming characteristics consisted of alternate photoresist lines and spaces arrays. Polysilicon lines with spacing-to-linewidth ratio on each side greater than 5 are referred to as isolated lines. The nested lines are commonly referred to as dense lines. The linewidth before trimming is often referred to as developed inspection critical dimension (DICD). After trimming, it is called the final inspection critical dimension (FICD). All the CD measurements were done using an in-line Hitachi scanning electron microscope (SEM). The trim rate was calculated by dividing the linewidth difference between the DICD and FICD by the trimming time. The trim rates were calculated over 13 points on each dice across the wafer.

The XPS measurements were performed ex situ on an Axis HSi spectrometer (Kratos Analytical Ltd., Manchester, Lancashire, UK) using a monochromatic Al–K_α X-ray source (1486.6 eV photons), at a constant dwell time of 100 ms and pass energy of 40 eV. The measurements were taken with the charge neutralizer on. The pressure in the analysis chamber was maintained at 5.0×10^{-8} Torr or lower during each measurement. The spectra of elements were curve-fitted by the software VISION 2.0 with Gaussian peaks to determine the relative atomic concentration of various bondings. After the energy shifts caused by charging of the photoresist surface, the required adjustments are made by using an internal reference provided by the C 1*s* level of the hydrocarbon peak, whose commonly adopted binding energy is 285.0 eV. XPS analysis was carried out in regions where the aforementioned line and space structure arrays spread over a distance in excess of the approximately 400×400-μm X-ray beam spot. Therefore, the photoelectrons detected by the analyzer represent contributions from many line and space features. The analysis of the resist sidewall was performed using the approach described by Oehrlein et al. (1989). The angle between the X-ray source and electron analyzer was fixed at 45°. The angle of 90° between the sample surface and the electron analyzer was used to analyze the top of the features and the bottom of the spaces. The sample was tilted to 60°, with respect to the axis of the electron analyzer, when the analyses of the top and sidewall of the features were done. The sample is tilted so that the trench bottom is not irradiated by the incident flux of X-ray because of intervening resist mask/polysilicon features and therefore no X-ray–induced photoelectron emission from the trench bottom will take place.

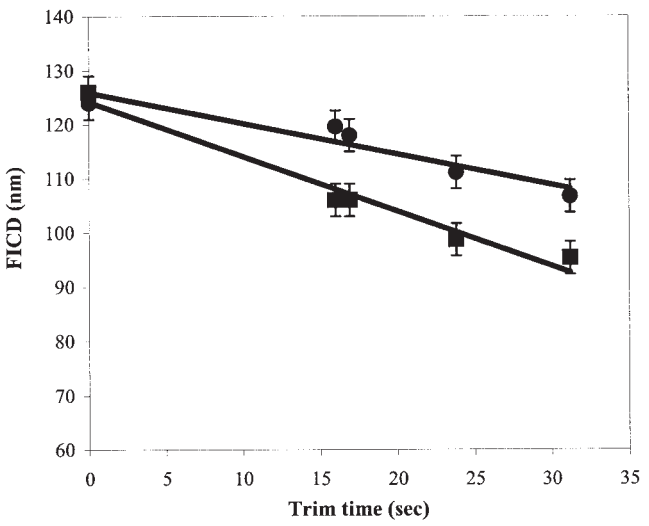

Figure 1. Final inspection critical dimension (FICD) of the photoresist as a function of trim time in the HBr/O_2 plasma for dense (●) and isolated (■) line, respectively.

All the trimming and etching were carried out at 70°C.

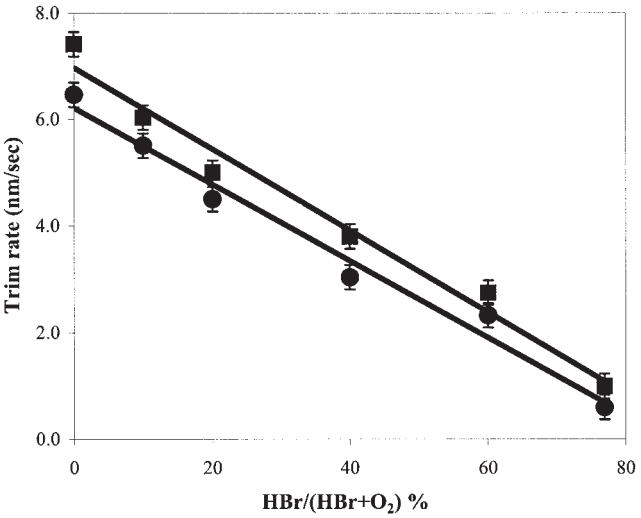

Figure 2. Trim rate of the photoresist at 70°C as a function of HBr percentage in the HBr/O_2 mixture for dense (●) and isolated (■) line, respectively.

Results

Trim rate

Trimming with HBr/O_2. Figure 1 shows the CD SEM-measured resist linewidth vs. trimming time when 100 sccm of HBr and 30 sccm of O_2 were used. The resist linewidth is a linearly decreasing function of trim time in the HBr/O_2 plasma. The trim rates are determined from Figure 1 as the slopes of the lines, which are 0.57 and 1.01 nm/s for dense and isolated lines, respectively. Figure 2 illustrates the dependency of trim rate as a function of HBr gas composition. The resist trim rate exhibits a nearly perfect linear variation with HBr gas flow percentage.

Trimming with Cl_2/O_2. Figure 3 displays the dependency of resist pattern length on trimming time at 100 sccm Cl_2 and 30 sccm O_2. Trimming proceeds at a rate of 0.26 and 0.38 nm/s for dense and isolated lines, respectively, as determined from Figure 3. Figure 4 exhibits the change in the trim rate at 70°C when the mixing ratio of Cl_2 to O_2 was varied. The trim rate decreases monotonically and rapidly with increasing Cl_2 gas flow.

Trimming with CF_4/O_2. Our previous study showed that the change in resist length is a linear function of trim time (Sin et al, 2002). Lateral trim rates of about 1.02 and 1.23 nm/s are observed for dense and isolated lines, respectively, at 100 sccm CF_4 and 30 sccm O_2. The effect of the CF_4 mixing ratio to O_2 on the trim rate is again exhibited as in Figure 5. Small amounts of CF_4 added to the oxygen plasma drastically en-

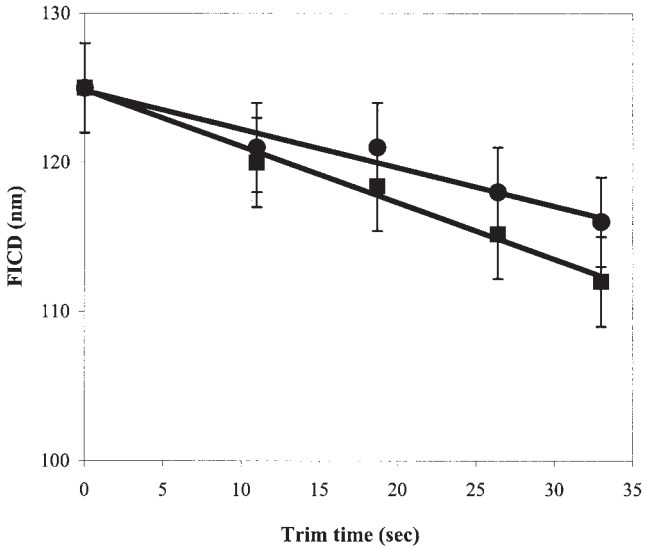

Figure 3. FICD of the photoresist as a function of trim time in the Cl_2/O_2 plasma for dense (●) and isolated (■) line, respectively.

All the trimming and etching were performed at 70°C.

hance the trim rate. With further increase in CF_4 addition, the trim rate goes through a maximum at about 12% CF_4 gas flow and then drops sharply.

Activation energy of resist trimming in different gas mixtures

The trim rate increases with increasing temperature for all three HBr/O_2, Cl_2/O_2, and CF_4/O_2 gas mixtures, suggesting a chemical reaction–activated process. Indeed, trim rate can be characterized by an Arrhenius expression. Arrhenius plots of the logarithm of trim rate vs. the reciprocal of the experiment temperature for various additive gases are plotted in Figure 6 for both dense and isolated lines. The

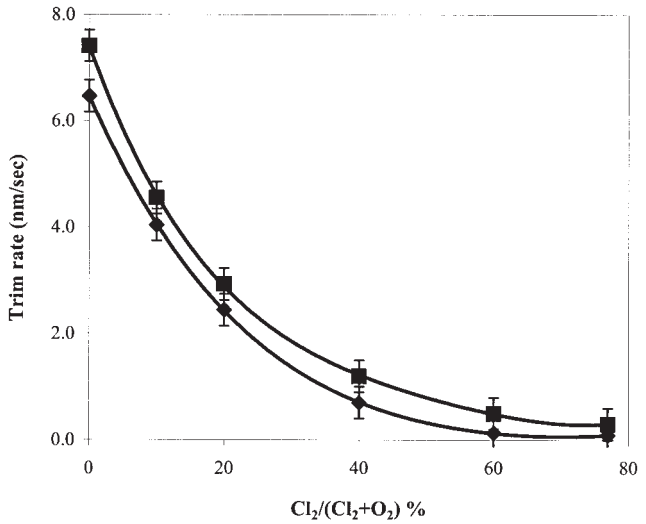

Figure 4. Trim rate of the photoresist at 70°C as a function of Cl_2 percentage in the Cl_2/O_2 mixture for dense (●) and isolated (■) line, respectively.

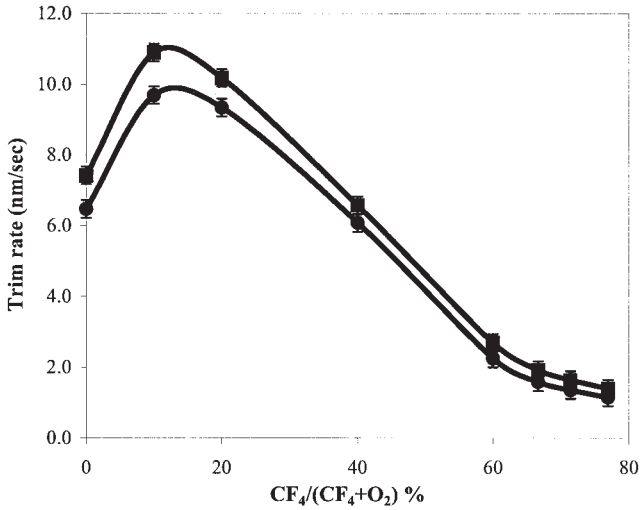

Figure 5. Trim rate of the photoresist at 70°C as a function of CF_4 percentage in the CF_4/O_2 mixture for dense (●) and isolated (■) line, respectively (Sin et al., 2002).

activation energy for each gas mixture is determined from the slope of the line and is indicated in the graph. Isolated lines (Figure 6b) tend to give the smaller activation energy than do dense lines (Figure 6a). In pure oxygen, the activation energy of the trimming reaction to the same resist is 0.072 and 0.082 eV for dense and isolated lines, respectively. With the addition of halogen gas to the pure oxygen plasma at 77% of gas mixture, which is the optimal operation condition, the activation energy of the reaction is increased. Resist trimming in Cl_2/O_2 plasma (1.62 and 0.8 eV for dense and isolated lines) has much higher activation energy than that in HBr/O_2 (0.38 and 0.14 eV for dense and isolated lines, respectively) and CF_4/O_2 (0.13 eV for both dense and isolated lines). For trimming with CF_4/O_2, dense and isolated lines give almost the same activation energy, which is about 0.13 eV. However, the activation energy of the dense line is about 2.7 and 2 times that of the isolated lines for HBr/O_2 and Cl_2/O_2 plasmas, respectively. The greater difference in the activation energies associated with dense and isolated lines may cause severe variation in the microloading effect, and indicate a more temperature-sensitive process. Therefore, it imposed a more difficult task for process control.

Dependency of polysilicon profiles on trimming chemistries

Figure 7 shows the micrographs of the resist profiles after trimming using HBr/O_2, Cl_2/O_2, and CF_4/O_2. All these chemistries give quite good vertical profiles of the resist. No distortion in the photoresist profile was observed during the trimming process. All the trimmed photoresist profiles demonstrate dimensions much smaller than those of the patterned features before trimming. Subsequently, the polysilicon gate electrode, with critical dimension less than 100 nm, was obtained using the trimmed photoresist as the etch mask in the following etch process by HBr/Cl_2 without breaking the vacuum in the same etcher. That is, the device of sub-100 nm can be fabricated

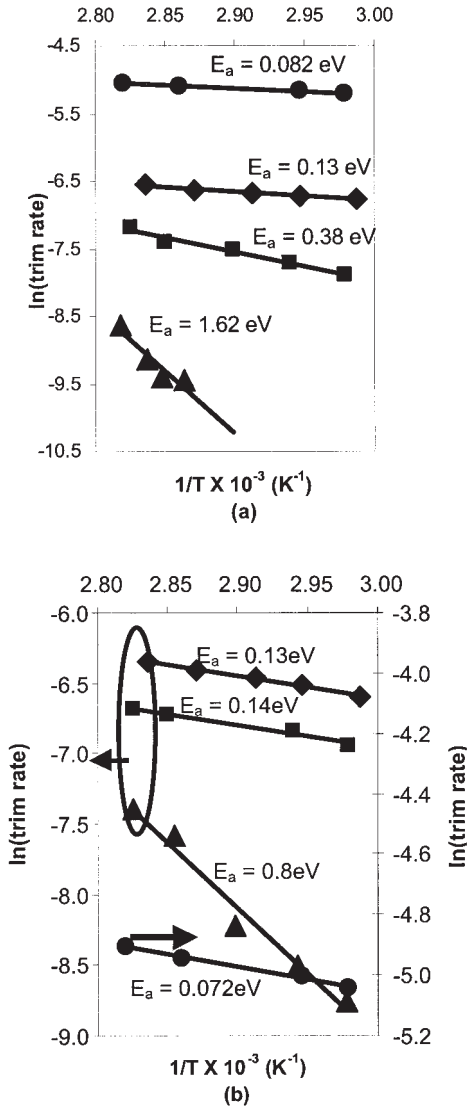

Figure 6. Activation energy of resist trimming for (a) dense lines and (b) isolated line in different gas mixture: O_2 (●), CF_4/O_2 (◆), HBr/O_2 (■), and Cl_2/O_2 (▲).

from the current 248-nm KrF lithography, which imposes the intrinsic limits of 0.18 or 0.13 μm if the optical proximity correction (OPC) could be used.

However, it has been observed that the dimension of the etched underlying polysilicon becomes wider than the top trimmed resist mask when the resist is trimmed by Cl_2/O_2 under certain conditions, although it is not observed when the resist is trimmed by HBr/O_2 or CF_4/O_2. The CD gain is more evident for dense lines. Figure 8 shows the SEM micrographs of the polysilicon with the trimmed resist mask still on top of it. A thick layer of deposition is visible on the polysilicon sidewall when the resist is trimmed with Cl_2/O_2 (Figure 8b). In contrast, it is thinner when the resist is trimmed with HBr/O_2 and CF_4/O_2. Another interesting artifact observed is the rough trench bottom of the etched polysilicon, as seen in Figure 8. This phenomenon is known as "grass formation" or micro-mask roughening (Mahorowala and Sawin, 2002). Polysilicon surface roughening is observed when the wafer is exposed previously to HBr/O_2 or Cl_2/O_2 during the resist trimming (Figures 8a and b), but it is less for HBr/O_2. Then again, surface roughening does not occur during polysilicon etching when the resist is trimmed with CF_4/O_2 (Figure 8c). "Grass formation" is observed under certain circumstances, where the redeposition rates are significant relative to etching rates and when the etching is driven by directional ion bombardment (van Roosmalen et al., 1991). If the redeposition is less severe, "cones" or "grass" can still be formed locally. The formation of cones is attributed to the high selectivity difference in etching rates between the uncovered substrate and the covered regions by redeposition. This shows that the trimming gas chemistry will affect the following etching steps by changing the conditions of the chamber wall (such as leaving Cl absorbed on the chamber wall), but the theory behind this is yet to be investigated.

XPS analysis of the resist sidewall after trimming

The results of the quantitative XPS analysis of the chemical concentrations on the feature sidewalls after trimming are summarized in Table 1. The quantitative coverage of carbon, oxygen, and halogen are derived from spectra recorded with the charge neutralizer on. After the energy shifts caused by charging of the photoresist surface, the required adjustments are made by using an internal reference provided by the C 1*s* level of the hydrocarbon peak, whose commonly adopted binding energy is 285.0 eV. The C 1*s* spectrum of the photoresist before trimming exhibits two resolved peaks, the C–C or C–H at 285.0 eV (Dilks, 1980), and a second peak at 286.4 eV, attributed to the carbon singly bonded to one oxygen (C–O bond) (Briggs and Seah, 1990).

The atomic concentrations of the different components detected on the resist sidewall in different plasma chemistries are given in Table 1. These results clearly demonstrate that Br gives the lowest percentage of halogen atomic concentration on the sidewall. On the contrary, F has the highest halogen atomic concentration percentage on the sidewall. The somewhat smaller Br coverage on the resist sidewall is also probably attributable to the presence of coadsorbed H and site blocking by the larger Br atoms, compared to F and Cl. Another interesting point observed is that the increasing trend on the relative elemental concentration of oxygen on the resist sidewall coincides with the sequence from Cl_2/O_2, HBr/O_2, to CF_4/O_2, which is also the order of increasing trim rate. The stoichiometry of the CO_yX_z film on the resist sidewall could not be accurately determined from the data in Table 1 because of the high C content from the bulk resist.

Qualitative analysis is carried out by fitting a series of peaks (based on the binding energies of the elemental and expected peaks of reaction products) to the measured C 1*s* photoelectron spectra (Figure 9). Figure 9 shows the C 1*s* spectra recorded on resist sidewall after trimming in HBr/O_2, Cl_2/O_2, and CF_4/O_2. All three C 1*s* spectra give the same number of bonds. They are C–C/C–H, C–O–X, X–C–O–X, and X_2–C–O–X (X = halogen). The intensities of the different carbon bonding components for each gas mixture are given in Table 2. Because the XPS analysis of blanket photoresist shows no halogen signal, the carbon–halogen signal must be coming from the CO_yX_z

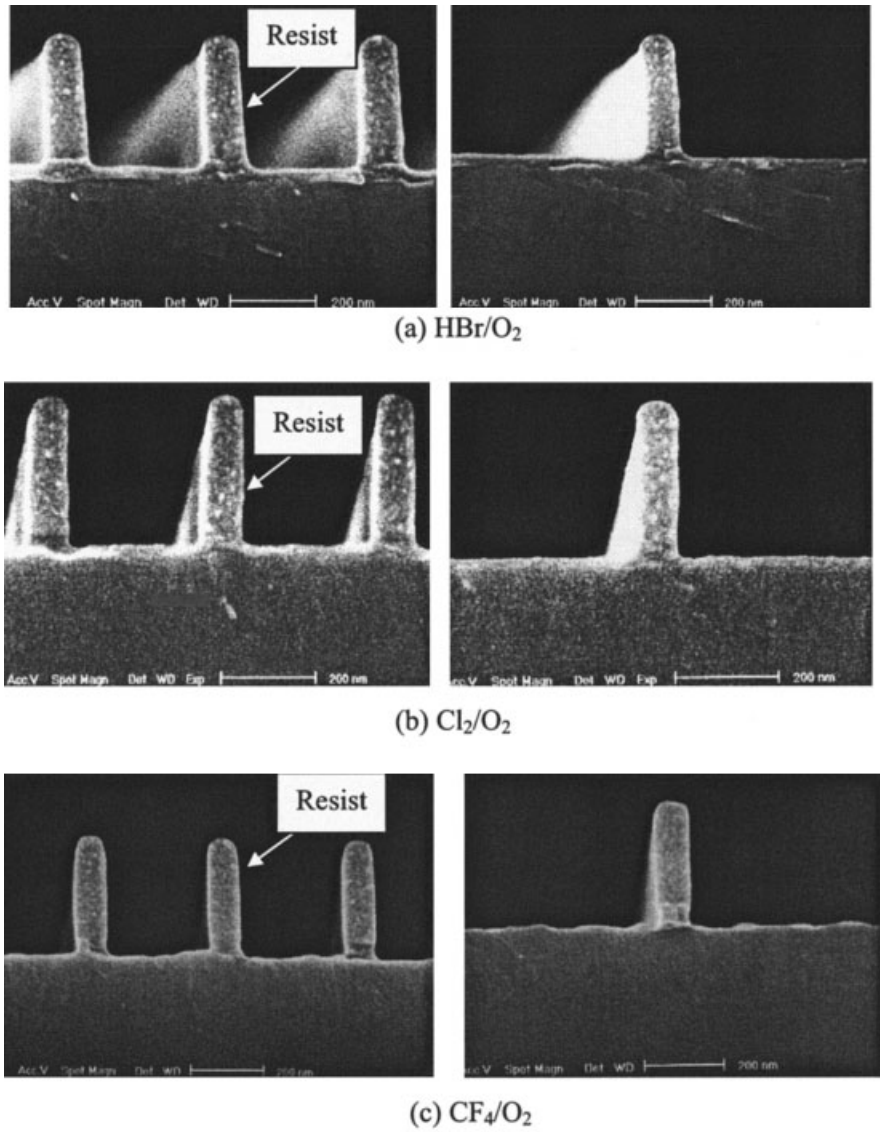

Figure 7. Cross-sectional SEM micrographs of the photoresist after trimming in (a) HBr/O_2, (b) Cl_2/O_2, and (c) CF_4/O_2 plasma.

No distortion on the resist profiles occurs after trimming.

polymer deposited on the resist sidewall during the trimming. All three halogen atoms, bromine and chlorine as well as fluorine, are electronegative and thus will induce shifts to higher binding energy by bonding to carbon directly.

Because of the higher electronegativity, fluorine induces a larger shift than with chlorine and bromine for the different components of the C 1*s* core level. Indeed, after the carbon spectra are curve-fitted using the Gaussian distribution, the C 1*s* components can be assigned as C–C/C–H (285.0 eV), C–O–F (286.5 eV), F–C–O–F (289.4eV), and F_2–C–O–F (292.3 eV binding energy) (Figure 9c). The deconvolution presented is in good agreement with a constant substitute effect for carbon directly attached to fluorine of 2.9 eV per single bond (Briggs and Seah, 1990). For resist trimming in Cl_2/O_2, the C–O–Cl peak at 286.6 eV, the Cl–C–O–Cl peak at 287.9 eV, and the Cl_2–C–O–Cl peak at 289.2 eV, as shown in Figure 9b, suggest that the addition of Cl directly to the carbon will induce a higher shift in binding energy of 1.3 eV. For trimming with HBr/O_2, the peaks are C–C/C–H (285.0 eV), C–O–Br (286.6 eV), Br–C–O–Br (287.7 eV), and Br_2–C–O–Br (288.8 eV) (Figure 9a). Bromine induces a small shift of approximately 1.1 eV by attaching directly to the carbon. The secondary effect of halogen (X) in C–O–X is small and is independent of the halogens (Briggs and Seah, 1990). Hence C–O–F, C–O–Cl, and C–O–Br have almost the same binding energies.

The intensities of the different carbon bonding components for each gas mixture are given in Table 2. Using the peaks arising from a carbon atom with at least one halogen bond, the relative occurrence of X_y–C–O–X ($y = 1$ or 2) to C–O–X was calculated. A higher relative amount of X_y–C–O–X bonds means that the carbon becomes more halogenated. Table 2 shows that the degree of halogenation (that is, the atomic concentration ratio of X_y–C–O–X/C–O–X) of the passivation film on the resist sidewall is the highest (1.47) when trimming

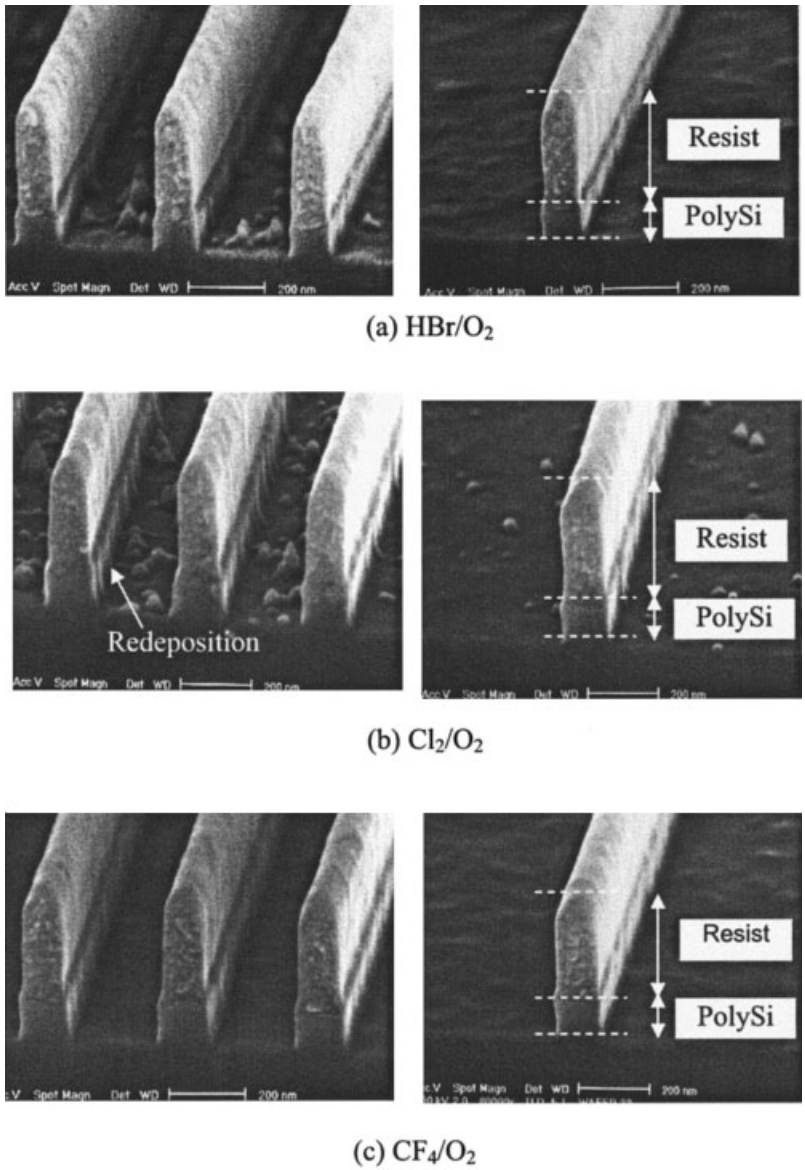

Figure 8. SEM micrographs of partially etched polysilicon with the photoresist as the mask on its top when the resist is trimmed with (a) HBr/O_2, (b) Cl_2/O_2, and (c) CF_4/O_2 plasma.

Rough polysilicon surface is observed when the wafer is previously exposed in HBr/O_2 or Cl_2/O_2 during the resist trimming.

in CF_4/O_2 and the lowest (1.07) in Cl_2/O_2. The previous data show that the resist trim rate decreases in the order of trimming in CF_4/O_2, HBr/O_2, and Cl_2/O_2. It is consistent that a more halogenated carbon film gives a higher trim rate.

It is worth mentioning that the atomic concentrations of these species are in proportion with the quantities of the XPS peak areas normalized by the corresponding sensitivity factors, not just the peak areas themselves. However, in this work, the sensitivity factors for the C 1*s* in these various bonds could be regarded as the same, in practice. Thus, the XPS peak area could be used directly as an indicator of the atomic concentrations of these species.

Table 1. Atomic Concentration Determined on the Resist Sidewall Trimmed Using Different Gas Chemistry

HBr/O_2	Br 3*d*	O 1*s*	C 1*s*
Atomic concentration (%)	1.96	19.73	77.54
Cl_2/O_2	Cl 2*p*	O 1*s*	C 1*s*
Atomic concentration (%)	14.46	14.96	70.58
CF_4/O_2	F 1*s*	O 1*s*	C 1*s*
Atomic concentration (%)	20.95	28.31	50.73

Discussion

All three two-component oxygen–halogen gas mixtures (that is, HBr/O_2, Cl_2/O_2, CF_4/O_2) show linear CD loss with trim time (Figures 1 and 3). That is, the trim rate is independent of the trim time. Trimming linearity is an important element for precise CD control. Because of the linearity, it is possible to adjust the trimming time based on each incoming wafer to obtain the desired final CD. At the same percentage of halogen additive, CF_4/O_2 gives the highest trim rate, followed by HBr/

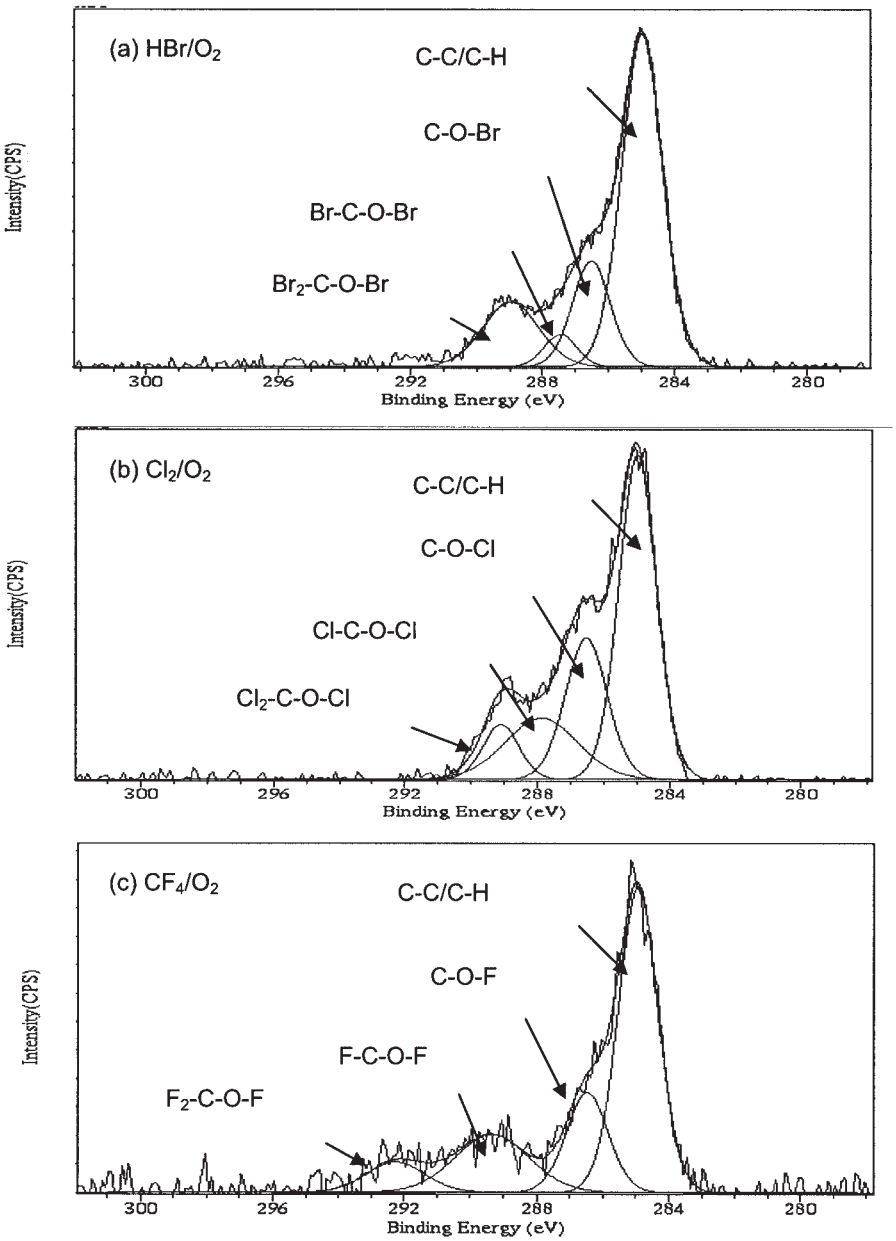

Figure 9. C 1*s* XPS spectra of the resist sidewall obtained at glancing angle under three different plasma chemistries: (a) HBr/O_2, (b) Cl_2/O_2, and (c) CF_4/O_2.

The peak at 285.0 eV arises from the bulk photoresist.

O_2, while trimming in Cl_2/O_2 has the lowest trim rate. The trim rate decreases monotonically with the increasing percentage of HBr and Cl_2 in the O_2 plasma (Figures 2 and 4), which can be attributed to sidewall passivation by bromine and chlorine compounds and dilution of oxygen concentration. However, the results are very different for CF_4/O_2, where the trim rate

Table 2. Area Percentage of the Different Components of the C 1*s* Gaussian Fitting Decomposition of XPS Photoresist Spectra for Three Gas Mixtures at Glancing Angle after Trimming

	Chemical Component				
	C–C/C–H	C–O–X	X–C–O–X	X_2–C–O–X	X_y–C–O–X/C–O–X*
Gas Chemistry	Amount of Area (%)				Degree of Halogenation
HBr/O_2 (X = Br)	61.16	18.00	4.71	16.14	1.16
Cl_2/O_2 (X = Cl)	49.81	24.23	18.22	7.74	1.07
CF_4/O_2 (X = F)	54.26	18.54	19.16	8.04	1.47

*The amount of X_y–C–O–X is the combined sum of X–C–O–X and X_2–C–O–X.

increases initially and then decreases with the further addition of CF_4 (Figure 5). The generalization that halogen reactivity decreases from F to Cl to Br clearly does not hold for the compounds investigated in this study under all trimming conditions. Sparks (1992) also reported that halogen reactivity did not strictly follow the trend of faster etch rates for F followed by Cl and then Br.

The effects of the addition of halogen gas on trimming can be considered as well on the basis of the sidewall passivation mechanism, plasma gas chemistry, and trimming reaction. In view of plasma chemistry, chlorine can remove the oxygen atom by forming stable halogen oxides (van Roosmalen et al., 1991) (that is, $Cl + O \rightarrow ClO$), resulting in decreases of reactive oxygen concentration in the plasma. Hence, the scavenging of reactive atomic oxygen when trimming with Cl_2/O_2 can explain the slow trim rate of Cl_2/O_2.

Nonetheless, because of the relatively higher bond strength of HBr than that of BrO, the removal of oxygen by formation of BrO is unlikely. With the addition of fluorine to O_2 plasma (such as CF_4/O_2) both trimming enhancement and fluorine passivation of the resist sidewall can occur. In the resist trimming process, a small amount of CF_4 addition enhances O_2 dissociation in plasma (Flamm et al., 1983) and increases the trim rate, accordingly. The increase in oxygen atom concentration can be explained by the higher electron density when CF_4 is added (Kushner et al., 1982), although at least part of the effect has been attributed to reactions between the excited oxygen molecules and the fluorocarbon radical species.

The initial increase in the trim rate with addition of CF_4 can also be caused by the active fluorine containing decomposition by-products, which accelerates the hydrogen extraction from the resist surface (Kataoka et al., 1999). This improves the efficiency of the resist oxidative decomposition reaction by producing sites that react rapidly with the molecular oxygen. Higher CF_4 concentrations, on the other hand, tend to passivate the trimmed surface with F and cover it by depositing the fluorinated polymers CO_xF_y (Sin et al. 2002). The decrease in trim rate with further addition of CF_4 is also attributed to the oxygen dilution by CF_4, and thus the trim rate decreases with high CF_4 addition.

Variation in activation energy is consistent with the variation in trim rate. Both dense and isolated lines, trimming using O_2 alone, have the lowest activation energy followed by that in CF_4/O_2 and HBr/O_2, whereas trimming with Cl_2/O_2 has the highest activation energy (Figure 6) at a halogen percentage of 77% in the mixture. This also happens to be the order of decreasing trim rate. The temperature effect on the trim rate includes the adsorption of the etchants, the chemical reaction on the surface, and the desorption of the products. The activation energy is different for different halogen-containing plasma chemistries, suggesting that halogen radicals are involved in the reaction of polymer oxidative decomposition. However, the activation energy of trimming for isolated lines is generally lower than that for dense lines. Compared to trimming in CF_4/O_2 and Cl_2/O_2, trimming in HBr/O_2 undergoes a substantial change in activation energy from dense to isolated lines, relative to dense line activation energy. The activation energy of dense lines is about 2.7 times that of activation energy of isolated lines.

Indeed, the difference in activation energy is reflected in the difference in trim rate between dense and isolated lines, also known as the *microloading effect*, which is a problem when one has to etch simultaneously densely packed features and isolated lines. Given that our previous work shows that trimming is a neutral-driven process (Sin et al., 2002), the trimming is affected by the neutral distribution in the line arrays. The much slower trim rate or higher activation energy of dense lines, relative to that of isolated lines, when trimming with HBr/O_2 may be caused by the depletion of active Br etchant species from the gas phase to the resist sidewall for the trimming reaction. Moreover, the difficulty of the etched products to be diffused out from the line arrays may be attributable to the microloading effects as well (Plummer et al, 2000). Interestingly, Desvoivres et al. (2001) found the tapered thickness of the SiO_2 passivation layers on the sidewall of the Si-gate features when etched in HBr/O_2 high-density plasmas. That is, the passivity is not uniform through the sidewall of the features. In addition, Cl_2 has been reported to render a very significant microloading effect in polysilicon gate etching for sub-0.25-μm–generation devices by using the Cl_2-based high-density plasmas (Armacost et al., 1999). This phenomenon is attributed to the limited supply of the Cl_2 reactive species into the line arrays on the wafer surface, although Cl_2 is much smaller than the feature dimensions ($\sim$0.25 μm).

XPS sidewall analyses show the formation of CO_xBr_y, CO_xCl_y, and CO_xF_y film on the resist sidewall (Figure 9) when trimming in HBr/O_2, Cl_2/O_2, and CF_4/O_2, respectively. Our previous study (Sin et al., 2002) showed that when trimming in CF_4/O_2, a higher trim rate is accompanied by a higher degree of fluorination of resist sidewall film. In this study, XPS analysis again shows that a more halogenated carbon film gives a higher trim rate. Using the peaks arising from a carbon atom with at least one halogen bond, the relative occurrence of C–O–X (X = F, Cl, or Br) among all the X_y–C–O–X (y = 1 or 2) bonds was calculated. A higher relative amount of X_y–C–O–X bonds means that the carbon becomes more halogenated. It is found that the trim rate shows the same trend as the increasing proportionality of X_y–C–O–X/C–O–X. The degree of halogenation is the highest when trimming with CF_4/O_2, followed by HBr/O_2 then Cl_2/O_2, which is also the decreasing order of trim rate.

Such formation of CO_xBr_y and CO_xCl_y passivation layer on the sidewall of resist was previously reported by Kure et al. (1991) and Tokashiki et al. (1993) when etching with the HBr/O_2 and Cl_2/O_2 mixed plasma, respectively. However, when trimming with HBr, the carbon-containing passivation layer can be removed by H, dissociated from HBr, by the formation of any of the volatile species that hydrogen can make with carbon (Simko et al., 1991), such as CH_3OBr. This may result in a thinner passivation layer on the resist sidewall and less protection of bulk resist from trimming in HBr/O_2 compared to that in Cl_2/O_2, and, hence, a faster trim rate.

Furthermore, the XPS analyses on the resist sidewall illustrate that the atomic oxygen amount is the highest on the resist sidewall when trimming with CF_4/O_2 and the lowest when trimming with Cl_2/O_2 (Table 2). It is also consistent with the decreasing trend of the trim rate and supports the fact that atomic oxygen is the dominant trimming species in the oxygen-based plasmas (Hartney et al., 1989; Joubert et al., 1989).

In resist oxidative decomposition, a carbon–hydrogen bond is first dissociated to produce a radical polymer species (Luongo, 1960). An oxygen molecule then reacts at this site to

form the peroxide radical. Halogen atoms can enhance the reaction by removing hydrogen atoms from the polymer by fast abstraction, and subsequently by allowing the peroxide to form, thus breaking the polymer chain into volatile fragments (Chou et al., 1986). The breakage is accompanied by an increasing degree of halogenation. Besides that, halogenation can supply the excess energy for promoting the production of volatile species from their precursor states. Also, the higher halogenation of surface carbon favors the formation of highly halogenated products. In fact, there is a higher probability of forming a volatile molecule when the halogenated carbon is fully coordinated. In contrast, whereas the halogenation supplies the energy for bond breakage and formation of volatile products, it depletes the available sites for oxygen attachment as well. The two counteracting effects can account for the observed change of the trim rate with halogen addition. As a result, the effect of halogen addition is a balance between the reaction enhancement by halogen, changes in plasma gas chemistry, competition of reaction sites between halogen and oxygen, and passivation formation.

No distortion on the resist profiles takes place after the resist trimming (Figure 7). All three gas mixtures give vertical resist profiles. Nonetheless, the subsequent polysilicon etching step is affected by the gas chemistries used for trimming because of different chamber conditions (Figure 8). For instance, CD gain is observed after polysilicon etching when the resist is trimmed previously with Cl_2/O_2 but insignificant when the resist is trimmed with HBr/O_2 and CF_4/O_2: this is caused by the thick deposition on the polysilicon sidewall, as seen in the SEM micrograph (Figure 8b). Also, the roughening of the polysilicon surface occurs for Cl_2/O_2 and HBr/O_2 trimming chemistry, but not for CF_4/O_2. Thus, the formation and the extent of this bumpy texture are sensitive to the types of the plasmas to which the substrate was previously exposed, and also depend on the reactor materials and the impurities (Flamm et al., 1983; Lehmann and Widmer, 1980).

The plasma chemistry used for polysilicon etching in this study is HBr/Cl_2. As mentioned earlier, when etching with HBr/O_2 or $Cl_2/HBr/O_2$ plasmas, or with addition of a small amount of oxygen to the Cl_2 plasma, the bottom of the polysilicon trenches became bumpy and the etch rates were nonuniform (Denton and Wallace, 1992; Desvoivres et al., 2001; Guinn et al., 1995; Lehmann and Widmer, 1980). Their XPS analyses reveal that the deposit is mainly either SiO_xCl_y or SiO_xBr_y. This implies that the oxygen remaining from the previous resist trimming step, acting as contaminant in the subsequent polysilicon etching, caused the surface roughening in this study.

The significant effect of the small oxygen concentrations on the polysilicon etching in HBr/Cl_2 is attributed to the large selectivity between polysilicon and the deposits by the oxygen plasma. However, the introduction of fluorine by CF_4 to a typical $HBr/Cl_2/O_2$ polysilicon etch process suppresses the formation of SiO_xBr_y or SiO_xCl_y by the formation of particularly volatile SiF_4 (Lill et al., 2001). This may explain why there is no deposition on the polysilicon surface when the resist is trimmed beforehand by CF_4/O_2. Bestwick et al. (1990) also reported that when gaseous oxygen is present during etching of polysilicon using HBr, either as a contaminant or intentionally, the silicon surface may become extensively oxidized and results in a rough surface. However, the result is different when fluorine is present. The extensive oxidation of the silicon surface does not occur until there is a high proportion of oxygen. The aforementioned redeposition of the halogen oxysilane occurs not only on the etched polysilicon surface itself, but also on its sidewall. Thus, the CD gain is attributed to the considerable redeposition to the polysilicon sidewall, which may be caused by the same materials as that deposited on the polysilicon surface.

Conclusions

The performance of the resist trimming process (that is, the trim rate and the vertical profiles) by the halogen–oxygen plasmas, HBr/O_2, Cl_2/O_2, and CF_4/O_2, was investigated. The angle-resolved XPS was also used to examine the constituents of the resist sidewall films in an attempt to study how the trim rate is influenced by the sidewall films formed during resist trimming. The results show that the trim rate is a constant with respect to the trim time. Trim rate decreases monotonically with increasing percentage of HBr and Cl_2 in the O_2 plasma. However, when trimming with CF_4/O_2, the trim rate increases initially with the addition of a small amount of CF_4 and then decreases with further addition of CF_4. Trimming in CF_4/O_2 has the highest trim rate, followed by HBr/O_2, then Cl_2/O_2 at the same percentage of halogen-containing gas in the mixture. All these chemistries give quite good vertical profiles of the resist.

Formation of CO_xF_y, CO_xCl_y, and CO_xBr_y passivation is detected on the resist sidewall. The XPS analysis also shows that a higher trim rate takes place with a larger atomic oxygen concentration and a greater degree of halogenation on the surface of the resist sidewall. It is suggested that halogen atoms can enhance the reaction by removing hydrogen atoms from the photoresist by fast abstraction and subsequently by allowing peroxide to form, thus breaking the polymer chain into volatile fragments. The breakage is accompanied by an increasing degree of halogenation. Different activation energies in different gas mixtures indicate that halogen radicals are involved in the reaction. Halogen radicals also play a part in plasma chemistry. Addition of fluorine can increase the efficiency of oxygen dissociation, whereas chlorine removes oxygen by formation of chlorine oxide. XPS analysis also reveals that the amount of oxygen on the resist sidewall is the highest when trimming with CF_4/O_2 and the lowest when trimming with Cl_2/O_2. Hence, trimming is a compromise among the reaction enhancement by halogen, changes in plasma gas chemistry, site-competition between halogen and oxygen, and sidewall passivation formation.

Acknowledgments

The authors thank the National University of Singapore and the Chartered Semiconductor Manufacturing Ltd. for financial support.

Literature Cited

Armacost, M., P. D. Hoh, R. Wise, W. Yan, J. J. Brown, J. H. Keller, G. A. Kaplita, S. D. Halle, K. P. Muller, M. D. Naeem, S. Srinivasan, H. Y. Ng, M. Gutsche, A. Gutmann, and B. Spuler, "Plasma-Etching Processes for ULSI Semiconductor Circuits," *IBM J. Res. Dev.*, **43**, 39 (1999).

Baker, D., T. Zheng, C. Takemoto, S. Sethi, C. Gabriel, and G. Scot, "0.12 Micron Logic Process Using 248 nm Step-and-Scan System," *Proc. SPIE 3999*, p. 294 (2000).

Bestwick, T. D., and G. S. Oehrlein, "Reactive Ion Etching of Silicon

Using Bromine Containing Plasmas," *J. Vac. Sci. Technol. A*, **8**, 1696 (1990).
Briggs, D., and M. P. Seah, *Practical Surface Analysis: Volume 1, Auger and X-ray Photelectron Spectroscopy*, 2nd ed., Wiley, New York, p. 444 (1990).
Burmester, R., J. Winnerl, and F. Neppl, "Realization of Deep-submicron MOSFETs by Lateral Etching," *Microelectron. Eng.*, **13**, 473 (1991).
Chou, N. J., J. Parazsczak, E. Babich, Y. S. Chaug, and R. Goldblatt, "Mechanism of Microwave Plasma Etching of Polymides in O_2 and CF_4 Gas Mixtures," *Microelectron. Eng.*, **5**, 375 (1986).
Chung, J., M.-C. Jeng, J. E. Moon, A. T. Wu, T. Y. Chan, P. K. Ko, and C. M. Hu, "Deep-submicrometer MOS Device Fabrication Using a Photoresist-Ashing Technique," *IEEE Electron. Device Lett.*, **9**(4), 186 (1988).
Denton, H. L., and R. M. Wallace, "Controlling Polymer Formation during Polysilicon Etching in a Magnetically Enhanced Reactive Ion Etcher," *Proc. SPIE 1803*, p. 36 (1992).
Desvoivres, L., L. Vallier, and O. Joubert, "X-ray Photoelectron Spectroscopy Investigation of Sidewall Passivation Films Formed during Gate Etch Processes," *J. Vac. Sci. Technol. B*, **19**, 420 (2001).
Dilks, A., *Electron Spectroscopy—Theory, Techniques and Applications*, C. R. Brundle and A. D. Baker, eds., Academic, London, Vol. 4, p. 277 (1980).
Doemling, M. F., N. R. Rueger, G. S. Oehrlein, and J. M. Cook, "Photoresist Erosion Studied in an Inductively Coupled Plasma Reactor Employing CHF_3," *J. Vac. Sci. Technol. B*, **16**, 1998 (1998).
Flamm, D. L., V. M. Donnelly, and D. E. Ibbotson, "Basic Chemistry and Mechanisms of Plasma Etching," *J. Vac. Sci. Technol. B*, **1**, 23 (1983).
Guinn, K. V., C. C. Cheng, and V. M. Donnelly, "Quantitative Chemical Topography of Polycrystalline Si Anisotropically Etched in Cl_2/O_2 High Density Plasmas," *J. Vac. Sci. Technol. B*, **13**, 214 (1995).
Hartney, M. A., D. W. Hess, and D. S. Soane, "Oxygen Plasma Etching for Resist Stripping and Multilayer Lithography," *J. Vac. Sci. Technol. B*, **7**, 1 (1989).
Hsu, K. C., and M. D. Koretsky, "Surface Kinetics of Polyphenylene Oxide Etching in a CF_4/O_2/Ar Downstream Microwave Plasma," *J. Electrochem. Soc.*, **147**, 1818 (2000).
Hutton, R. S., C. H. Boyce, and G. N. Taylor, "Plasma Development of a Silylated Bilayer Resist: Effects of Etch Chemistry on Critical Dimension Control and Feature Profiles," *J. Vac. Sci. Technol. B*, **13**, 2366 (1995).
Joubert, O., J. Pelletier, and Y. Arnal, "The Etching of Polymers in Oxygen-Based Plasmas: A Parametric Study," *J. Appl. Phys.*, **65**, 5096 (1989).
Kataoka, Y., S. Saito, and K. Omiya, "Effect of CF_4 Addition on Downflow Ashing under Atmospheric Pressure," *Jpn. J. Appl. Phys.*, **38**, 3731 (1999).
Keller, J. H., "Inductive Plasmas for Plasma Processing," *Plasma Sources Sci. Technol.*, **5**, 166 (1996).
Kure, T., H. Kawakami, S. Tachi, and H. Enami, "Low-Temperature Etching of Deep-Submicron Trilayer Resist," *Jpn. J. Appl Phys.*, **30**, 1562 (1991).
Kushner, M., "A Kinetic Study of the Plasma-Etching Process. II. Probe Measurements of Electron Properties in an RF Plasma-Etching Reactor," *J. Appl. Phys.* **53**, 2939 (1982).
Lee, W. W., Q. He, M. Hanratty, D. Rogers, A. Chatterjee, R. Kraft, and R. A. Champman, "Fabrication of 0.06 μm Poly-Si Gate Using DUV Lithography with A Designed $Si_xO_yN_z$ film as an ARC and Hardmask," *1997 Symposium on VLSI Technology Digest of Technical Papers*, 131 (1997).
Lehmann, H. W., and R. Widmer, "Dry Etching for Pattern Transfer," *J. Vac. Sci. Technol.*, **17**, 1177 (1980).
Li, X., X. Hua, G. S. Oehrlein, M. Barela, and H. M. Anderson, "Fluorocarbon-Based Plasma Etching of SiO_2: Comparison of C_4F_6/Ar and C_4F_8/Ar Discharges," *J. Vac. Sci. Technol. A*, **20**, 2052 (2002).
Lill, T., F. Ameri, S. Deshmukh, D. Podlesnik, L. Vallier, and O. Joubert, "Sidewall Passivation Mechanism of CF_4 Added Polysilicon Gate Etch Process," Paper presented at AVS 48th International Conference, unpublished (2001).
Luongo, J. P., "Infrared Study of Oxygenated Groups Formed in Polyethylene during Oxidation," *J. Polym. Sci.*, **42**, 139 (1960).
Mahorowala, A., and H. H. Sawin, "Etching of Polysilicon in an Inductively Coupled Cl_2 and HBr Discharges: I. Experimental Characterization of Polysilicon Profiles," unpublished (2002).
Nakao, S., J. Itoh, A. Nakae, I. Kanai, T. Saitoh, H. Matsubara, K. Tsujita, I. Arimoto, and W. Wakamiya, "Extension of KrF Lithography to Sub-50 nm Pattern Formation," *Proc. SPIE 4000*, 358 (2000).
Oehrlein, G.S., K. K. Chan, M. A. Jaso, and G. W. Rubloff, "Surface Analysis of Realistic Semiconductor Microstructures," *J. Vac. Sci. Technol. A*, **7**, 1030 (1989).
Ono, M., M. Saito, and T. Yoshitomi, "Fabrication of Sub-50-nm Gate Length *n*-Metal–Oxide–Semiconductor Field Effect Transistors and Their Electrical Characteristics," *J. Vac. Sci. Technol. B*, **13**, 1740 (1995).
Peters, L., "Industry Confronts Sub-100 nm Challenges," *Semiconductor Int.*, **26**(1), 42 (2003).
Plummer, J. D., M. Deal, and P. B. Griffin, *Silicon VLSI Technology: Fundamentals, Practice and Modeling*, Prentice Hall, Upper Saddle River, NJ (2000).
Pons, M., J. Pelletier, and O. Joubert, "Anisotropic Etching of Polymers in SO_2/O_2 Plasmas: Hypotheses on Surface Mechanisms," *J. Appl. Phys.*, **75**, 4709 (1994).
Simko, J. P., G. S. Oehrlein, and T. M. Mayer. "Removal of Fluorocarbon Residues on CF_4/H_2 Reactive-Ion-Etched Silicon Surfaces Using a Hydrogen Plasma," *J. Electrochem. Soc.*, **138**, 277 (1991).
Sin, C. Y., B.-H. Chen, W. L. Loh, J. Yu, P. Yelehanka, and L. Chan, "Resist Trimming Technique in CF_4/O_2 High-Density Plasmas for Sub-0.1-μm MOSFET Fabrication Using the 248-nm Lithography," *Microelectron. Eng.*, **65**(4), 394 (2003).
Sin, C. Y., B.-H. Chen, W. L. Loh, J. Yu, P. Yelehanka, A. See, and L. Chan, "Resist Trimming in High-Density CF_4/O_2 Plasmas for Sub-0.1-μm Device Fabrication," *J. Vac. Sci. Technol. B*, **20**, 1974 (2002).
Sparks, D. R., "Plasma Etching of Si, SiO_2, Si_3N_4, and Resist with Fluorine, Chlorine, and Bromine Compounds," *J. Electrochem. Soc.*, **139**, 1736 (1992).
Tokashiki, K., K. Sato, N. Aoto, and E. Ikawa, "Multilayer Resist Dry Etching Technology for Deep Submicron Lithography," *J. Vac. Sci. Technol. B*, **11**, 2284 (1993).
Van Roosmalen, A. J., J. A. G. Baggerman, and S. J. H. Brader, *Dry Etching for VLSI*, Plenum Press, New Brunswick, NJ (1991).

Manuscript received May 19, 2003, and revision received Oct. 7, 2003.